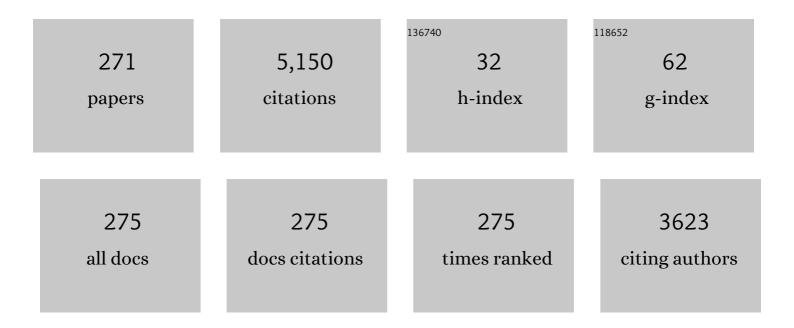
List of Publications by Year in descending order

Source: https://exaly.com/author-pdf/7405848/publications.pdf Version: 2024-02-01



#	Article	IF	CITATIONS
1	Recommended Methods to Study Resistive Switching Devices. Advanced Electronic Materials, 2019, 5, 1800143.	2.6	452
2	Coexistence of Grainâ€Boundariesâ€Assisted Bipolar and Threshold Resistive Switching in Multilayer Hexagonal Boron Nitride. Advanced Functional Materials, 2017, 27, 1604811.	7.8	229
3	Impact of Temperature on the Resistive Switching Behavior of Embedded \$hbox{HfO}_{2}*Based RRAM Devices. IEEE Transactions on Electron Devices, 2011, 58, 3124-3131.	1.6	201
4	Model for the Resistive Switching Effect in \$ hbox{HfO}_{2}\$ MIM Structures Based on the Transmission Properties of Narrow Constrictions. IEEE Electron Device Letters, 2010, 31, 609-611.	2.2	166
5	Silicon Oxide (SiO <i>_x</i>): A Promising Material for Resistance Switching?. Advanced Materials, 2018, 30, e1801187.	11.1	156
6	Resistive switching in hafnium dioxide layers: Local phenomenon at grain boundaries. Applied Physics Letters, 2012, 101, .	1.5	152
7	Quantum-size effects in hafnium-oxide resistive switching. Applied Physics Letters, 2013, 102, 183505.	1.5	151
8	Voltage and Power-Controlled Regimes in the Progressive Unipolar RESET Transition of HfO2-Based RRAM. Scientific Reports, 2013, 3, 2929.	1.6	135
9	Analytic Model for the Surface Potential and Drain Current in Negative Capacitance Field-Effect Transistors. IEEE Transactions on Electron Devices, 2010, 57, 2405-2409.	1.6	128
10	Standards for the Characterization of Endurance in Resistive Switching Devices. ACS Nano, 2021, 15, 17214-17231.	7.3	128
11	A Model for the Set Statistics of RRAM Inspired in the Percolation Model of Oxide Breakdown. IEEE Electron Device Letters, 2013, 34, 999-1001.	2.2	122
12	Electron transport through broken down ultra-thin SiO2 layers in MOS devices. Microelectronics Reliability, 2004, 44, 1-23.	0.9	108
13	Soft breakdown conduction in ultrathin (3-5 nm) gate dielectrics. IEEE Transactions on Electron Devices, 2000, 47, 82-89.	1.6	103
14	Cycle-to-Cycle Intrinsic RESET Statistics in \${m HfO}_{2}\$-Based Unipolar RRAM Devices. IEEE Electron Device Letters, 2013, 34, 623-625.	2.2	101
15	A function-fit model for the soft breakdown failure mode. IEEE Electron Device Letters, 1999, 20, 265-267.	2.2	76
16	Are soft breakdown and hard breakdown of ultrathin gate oxides actually different failure mechanisms?. IEEE Electron Device Letters, 2000, 21, 167-169.	2.2	65
17	Simulation of thermal reset transitions in resistive switching memories including quantum effects. Journal of Applied Physics, 2014, 115, .	1.1	61
18	Soft breakdown fluctuation events in ultrathin SiO2 layers. Applied Physics Letters, 1998, 73, 490-492.	1.5	60

#	Article	IF	CITATIONS
19	Multi-scale quantum point contact model for filamentary conduction in resistive random access memories devices. Journal of Applied Physics, 2014, 115, .	1.1	54
20	Impact of Intercell and Intracell Variability on Forming and Switching Parameters in RRAM Arrays. IEEE Transactions on Electron Devices, 2015, 62, 2502-2509.	1.6	52
21	Model for multi-filamentary conduction in graphene/hexagonal-boron-nitride/graphene based resistive switching devices. 2D Materials, 2017, 4, 025099.	2.0	51
22	A simple drain current model for Schottky-barrier carbon nanotube field effect transistors. Nanotechnology, 2007, 18, 025201.	1.3	50
23	Electrical characterization and modeling of pulse-based forming techniques in RRAM arrays. Solid-State Electronics, 2016, 115, 17-25.	0.8	47
24	The Quantum Point-Contact Memristor. IEEE Electron Device Letters, 2012, 33, 1474-1476.	2.2	46
25	\$\${ SIM}^2{ RRAM}\$\$ S I M 2 R R A M : a physical model for RRAM devices simulation. Journal of Computational Electronics, 2017, 16, 1095-1120.	1.3	45
26	Nonlinear conductance quantization effects in CeOx/SiO2-based resistive switching devices. Applied Physics Letters, 2012, 101, .	1.5	43
27	Set statistics in conductive bridge random access memory device with Cu/HfO2/Pt structure. Applied Physics Letters, 2014, 105, .	1.5	42
28	Compact Model for the Major and Minor Hysteretic <i>l–V</i> Loops in Nonlinear Memristive Devices. IEEE Nanotechnology Magazine, 2015, 14, 787-789.	1.1	42
29	Modeling the breakdown spots in silicon dioxide films as point contacts. Applied Physics Letters, 1999, 75, 959-961.	1.5	41
30	Point contact conduction at the oxide breakdown of MOS devices. , 0, , .		40
31	On the Thermal Models for Resistive Random Access Memory Circuit Simulation. Nanomaterials, 2021, 11, 1261.	1.9	39
32	n-Monotone exact functionals. Journal of Mathematical Analysis and Applications, 2008, 347, 143-156.	0.5	37
33	On the role of Ti adlayers for resistive switching in HfO2-based metal-insulator-metal structures: Top versus bottom electrode integration. Journal of Vacuum Science and Technology B:Nanotechnology and Microelectronics, 2011, 29, 01AD02.	0.6	37
34	Analytic modeling of leakage current through multiple breakdown paths in SiO/sub 2/ films. , 0, , .		34
35	Impact of the precursor chemistry and process conditions on the cell-to-cell variability in 1T-1R based HfO2 RRAM devices. Scientific Reports, 2018, 8, 11160.	1.6	33
36	A comprehensive analysis on progressive reset transitions in RRAMs. Journal Physics D: Applied Physics, 2014, 47, 205102.	1.3	31

3

#	Article	IF	CITATIONS
37	Voltage-Driven Hysteresis Model for Resistive Switching: SPICE Modeling and Circuit Applications. IEEE Transactions on Computer-Aided Design of Integrated Circuits and Systems, 2017, 36, 2044-2051.	1.9	31
38	Quantum Conductance in Memristive Devices: Fundamentals, Developments, and Applications. Advanced Materials, 2022, 34, e2201248.	11.1	31
39	Atomic layer deposited (TiO2)x(Al2O3)1â^²x/In0.53Ga0.47As gate stacks for III-V based metal-oxide-semiconductor field-effect transistor applications. Applied Physics Letters, 2012, 100, 062905.	1.5	30
40	Resistive switching in CeO2/La0.8Sr0.2MnO3 bilayer for non-volatile memory applications. Microelectronic Engineering, 2015, 147, 37-40.	1.1	30
41	Memristors for Neuromorphic Circuits and Artificial Intelligence Applications. Materials, 2020, 13, 938.	1.3	29
42	Model for the voltage and temperature dependence of the soft breakdown current in ultrathin gate oxides. Journal of Applied Physics, 2005, 97, 014104.	1.1	27
43	Volume Resistive Switching in metallic perovskite oxides driven by the Metal-Insulator Transition. Journal of Electroceramics, 2017, 39, 185-196.	0.8	26
44	Analysis and simulation of the multiple resistive switching modes occurring in HfO <i>x</i> -based resistive random access memories using memdiodes. Journal of Applied Physics, 2019, 125, .	1.1	26
45	Detection and fitting of the soft breakdown failure mode in MOS structures. Solid-State Electronics, 1999, 43, 1801-1805.	0.8	24
46	Resistive Switching with Self-Rectifying Tunability and Influence of the Oxide Layer Thickness in Ni/HfO2/n+-Si RRAM Devices. IEEE Transactions on Electron Devices, 2017, 64, 3159-3166.	1.6	24
47	Multivariate analysis and extraction of parameters in resistive RAMs using the Quantum Point Contact model. Journal of Applied Physics, 2018, 123, .	1.1	22
48	Experimental study of the series resistance effect and its impact on the compact modeling of the conduction characteristics of HfO2-based resistive switching memories. Journal of Applied Physics, 2021, 130, .	1.1	22
49	Degradation of high-K LA2O3 gate dielectrics using progressive electrical stress. Microelectronics Reliability, 2005, 45, 1365-1369.	0.9	21
50	Equivalent circuit modeling of the bistable conduction characteristics in electroformed thin dielectric films. Microelectronics Reliability, 2015, 55, 1-14.	0.9	21
51	Soft Breakdown in Ultrathin SiO2Layers: the Conduction Problem from a New Point of View. Japanese Journal of Applied Physics, 1999, 38, 2223-2226.	0.8	20
52	Monitoring the degradation that causes the breakdown of ultrathin (<5 nm) SiO ₂ gate oxides. IEEE Electron Device Letters, 2000, 21, 251-253.	2.2	20
53	Failure physics of ultra-thin SiO2gate oxides near their scaling limit. Semiconductor Science and Technology, 2000, 15, 445-454.	1.0	20
54	Multilevel recording in Bi-deficient Pt/BFO/SRO heterostructures based on ferroelectric resistive switching targeting high-density information storage in nonvolatile memories. Applied Physics Letters, 2013, 103, .	1.5	20

#	Article	IF	CITATIONS
55	Relationship among Current Fluctuations during Forming, Cell-To-Cell Variability and Reliability in RRAM Arrays. , 2015, , .		20
56	Investigation on the Conductive Filament Growth Dynamics in Resistive Switching Memory via a Universal Monte Carlo Simulator. Scientific Reports, 2017, 7, 11204.	1.6	20
57	Switching Voltage and Time Statistics of Filamentary Conductive Paths in HfO ₂ -Based ReRAM Devices. IEEE Electron Device Letters, 2018, 39, 656-659.	2.2	20
58	Tailoring the Switching Dynamics in Yttrium Oxideâ€Based RRAM Devices by Oxygen Engineering: From Digital to Multiâ€Level Quantization toward Analog Switching. Advanced Electronic Materials, 2020, 6, 2000439.	2.6	20
59	Modeling of Short-Term Synaptic Plasticity Effects in ZnO Nanowire-Based Memristors Using a Potentiation-Depression Rate Balance Equation. IEEE Nanotechnology Magazine, 2020, 19, 609-612.	1.1	20
60	SPICE Implementation of the Dynamic Memdiode Model for Bipolar Resistive Switching Devices. Micromachines, 2022, 13, 330.	1.4	20
61	Effects of Ti incorporation on the interface properties and band alignment of HfTaOx thin films on sulfur passivated GaAs. Applied Physics Letters, 2011, 98, 022901.	1.5	19
62	Multi-channel conduction in redox-based resistive switch modelled using quantum point contact theory. Applied Physics Letters, 2013, 103, .	1.5	19
63	Application of the Quasi-Static Memdiode Model in Cross-Point Arrays for Large Dataset Pattern Recognition. IEEE Access, 2020, 8, 202174-202193.	2.6	19
64	Connectome of memristive nanowire networks through graph theory. Neural Networks, 2022, 150, 137-148.	3.3	19
65	Post soft breakdown conduction in SiO/sub 2/ gate oxides. , 0, , .		18
66	Effects of high-field electrical stress on the conduction properties of ultrathin La2O3 films. Applied Physics Letters, 2005, 86, 232104.	1.5	18
67	Formation and Characterization of Filamentary Current Paths in \$hbox{HfO}_{2}\$-Based Resistive Switching Structures. IEEE Electron Device Letters, 2012, 33, 1057-1059.	2.2	18
68	Modeling of the Hysteretic \$I{-}V\$ Characteristics of \${m TiO}_{2}\$-Based Resistive Switches Using the Generalized Diode Equation. IEEE Electron Device Letters, 2014, 35, 390-392.	2.2	18
69	Characterization of HfO 2 -based devices with indication of second order memristor effects. Microelectronic Engineering, 2018, 195, 101-106.	1.1	18
70	Mesoscopic approach to the soft breakdown failure mode in ultrathin SiO2 films. Applied Physics Letters, 2001, 78, 225-227.	1.5	17
71	Post-radiation-induced soft breakdown conduction properties as a function of temperature. Applied Physics Letters, 2001, 79, 1336-1338.	1.5	17
72	A diodelike conduction model for the postbreakdown current in metal–oxide–semiconductor structures. Journal of Applied Physics, 2004, 96, 6940-6942.	1.1	17

#	Article	IF	CITATIONS
73	Initial leakage current related to extrinsic breakdown in HfO2/Al2O3 nanolaminate ALD dielectrics. Microelectronic Engineering, 2011, 88, 1380-1383.	1.1	17
74	Statistical model for radiation-induced wear-out of ultra-thin gate oxides after exposure to heavy ion irradiation. IEEE Transactions on Nuclear Science, 2003, 50, 2167-2175.	1.2	16
75	Statistical characteristics of reset switching in Cu/HfO2/Pt resistive switching memory. Nanoscale Research Letters, 2014, 9, 2500.	3.1	16
76	A physical compact DC drain current model for long-channel undoped ultra-thin body (UTB) SOI and asymmetric double-gate (DG) MOSFETs with independent gate operation. Solid-State Electronics, 2011, 57, 61-66.	0.8	15
77	Modeling the breakdown statistics of Al2O3/HfO2 nanolaminates grown by atomic-layer-deposition. Solid-State Electronics, 2012, 71, 48-52.	0.8	15
78	A Physical Model for the Statistics of the Set Switching Time of Resistive RAM Measured With the Width-Adjusting Pulse Operation Method. IEEE Electron Device Letters, 2015, 36, 1303-1306.	2.2	15
79	Study From Cryogenic to High Temperatures of the High- and Low-Resistance-State Currents of ReRAM Ni–HfO ₂ –Si Capacitors. IEEE Transactions on Electron Devices, 2016, 63, 1877-1883.	1.6	15
80	Effect of the voltage ramp rate on the set and reset voltages of ReRAM devices. Microelectronic Engineering, 2017, 178, 61-65.	1.1	15
81	Analysis and control of the intermediate memory states of RRAM devices by means of admittance parameters. Journal of Applied Physics, 2018, 124, .	1.1	15
82	Switching behavior of the soft breakdown conduction characteristic in ultra-thin (<5 nm) oxide MOS capacitors. , 1998, , .		14
83	A strong analogy between the dielectric breakdown of high-K gate stacks and the progressive breakdown of ultrathin oxides. Journal of Applied Physics, 2011, 109, 124115.	1.1	14
84	DC and low-frequency noise behavior of the conductive filament in bipolar HfO2-based resistive random access memory. Microelectronic Engineering, 2013, 107, 1-5.	1.1	14
85	Threshold Switching and Conductance Quantization in Al/HfO ₂ /Si(p) Structures. Japanese Journal of Applied Physics, 2013, 52, 04CD06.	0.8	14
86	Memristive State Equation for Bipolar Resistive Switching Devices Based on a Dynamic Balance Model and Its Equivalent Circuit Representation. IEEE Nanotechnology Magazine, 2020, 19, 837-840.	1.1	14
87	Analysis of the degradation and breakdown of thin SiO/sub 2/ films under static and dynamic tests using a two-step stress procedure. IEEE Transactions on Electron Devices, 2000, 47, 2138-2145.	1.6	13
88	BREAKDOWN MODES AND BREAKDOWN STATISTICS OF ULTRATHIN SiO2 GATE OXIDES. International Journal of High Speed Electronics and Systems, 2001, 11, 789-848.	0.3	13
89	Degradation dynamics of ultrathin gate oxides subjected to electrical stress. IEEE Electron Device Letters, 2003, 24, 604-606.	2.2	13
90	Effects of the electrical stress on the conduction characteristics of metal gate/MgO/InP stacks. Microelectronics Reliability, 2009, 49, 1052-1055.	0.9	13

#	Article	IF	CITATIONS
91	(Invited) Elucidating the Origin of Resistive Switching in Ultrathin Hafnium Oxides through High Spatial Resolution Tools. ECS Transactions, 2014, 64, 19-28.	0.3	13
92	Modeling of hysteretic Schottky diode-like conduction in Pt/BiFeO3/SrRuO3 switches. Applied Physics Letters, 2014, 105, .	1.5	13
93	Temperature and polarity dependence of the switching behavior of Ni/HfO2-based RRAM devices. Microelectronic Engineering, 2015, 147, 75-78.	1.1	13
94	Analysis on the Filament Structure Evolution in Reset Transition of Cu/HfO2/Pt RRAM Device. Nanoscale Research Letters, 2016, 11, 269.	3.1	13
95	Study of the admittance hysteresis cycles in TiN/Ti/HfO2/W-based RRAM devices. Microelectronic Engineering, 2017, 178, 30-33.	1.1	13
96	Comparative study of the breakdown transients of thin Al2O3 and HfO2 films in MIM structures and their connection with the thermal properties of materials. Journal of Applied Physics, 2017, 121, 094102.	1.1	13
97	Compact Modeling of the I-V Characteristics of ZnO Nanowires Including Nonlinear Series Resistance Effects. IEEE Nanotechnology Magazine, 2020, 19, 297-300.	1.1	13
98	A New Perspective Towards the Understanding of the Frequency-Dependent Behavior of Memristive Devices. IEEE Electron Device Letters, 2021, 42, 565-568.	2.2	13
99	Method for extracting series resistance in MOS devices using Fowler-Nordheim plot. Electronics Letters, 2004, 40, 1153.	0.5	12
100	Equivalent Circuit Model for the Gate Leakage Current in Broken Down \$hbox{HfO}_{2}/hbox{TaN/TiN}\$ Gate Stacks. IEEE Electron Device Letters, 2008, 29, 1353-1355.	2.2	12
101	An extension of the Curie-von Schweidler law for the leakage current decay in MIS structures including progressive breakdown. Microelectronics Reliability, 2011, 51, 1535-1539.	0.9	12
102	Analytic expression for the Fowler–Nordheim V–l characteristic including the series resistance effect. Solid-State Electronics, 2011, 61, 93-95.	0.8	12
103	Degradation analysis and characterization of multifilamentary conduction patterns in high-field stressed atomic-layer-deposited TiO2/Al2O3 nanolaminates on GaAs. Journal of Applied Physics, 2012, 112, 064113.	1.1	12
104	Study on the Connection Between the Set Transient in RRAMs and the Progressive Breakdown of Thin Oxides. IEEE Transactions on Electron Devices, 2019, 66, 3349-3355.	1.6	12
105	Switching events in the soft breakdown l–t characteristic of ultra-thin SiO2 layers. Microelectronics Reliability, 1999, 39, 161-164.	0.9	11
106	A new approach to analyze the degradation and breakdown of thin SiO2 films under static and dynamic electrical stress. IEEE Electron Device Letters, 1999, 20, 317-319.	2.2	11
107	Gate stack insulator breakdown when the interface layer thickness is scaled toward zero. Applied Physics Letters, 2010, 97, .	1.5	11
108	Compact Modeling of Complementary Resistive Switching Devices Using Memdiodes. IEEE Transactions on Electron Devices, 2019, 66, 2831-2836.	1.6	11

#	Article	IF	CITATIONS
109	Minimization of the Line Resistance Impact on Memdiode-Based Simulations of Multilayer Perceptron Arrays Applied to Pattern Recognition. Journal of Low Power Electronics and Applications, 2021, 11, 9.	1.3	11

Relation between defect generation, stress induced leakage current and soft breakdown in thin (<5) Tj ETQq0 0 0 rgBT /Overlock 10 Tf $\frac{10}{10}$

111	Modeling of the l–V characteristics of high-field stressed MOS structures using a Fowler–Nordheim-type tunneling expression. Microelectronics Reliability, 2002, 42, 935-941.	0.9	10
112	Quantum point contact model of filamentary conduction in resistive switching memories. , 2012, , .		10
113	Three-state resistive switching in HfO2-based RRAM. Solid-State Electronics, 2014, 98, 38-44.	0.8	10
114	Experimental Observation of Negative Susceptance in HfO ₂ -Based RRAM Devices. IEEE Electron Device Letters, 2017, 38, 1216-1219.	2.2	10
115	Coherent choice functions, desirability and indifference. Fuzzy Sets and Systems, 2018, 341, 1-36.	1.6	10
116	Nanoâ€Memristors with 4ÂmVÂSwitching Voltage Based on Surfaceâ€Modified Copper Nanoparticles. Advanced Materials, 2022, 34, e2201197.	11.1	10
117	A common framework for soft and hard breakdown in ultrathin oxides based on the theory of point contact conduction. Microelectronic Engineering, 1999, 48, 171-174.	1.1	9
118	Tunneling in sub-5nm La2O3 films deposited by E-beam evaporation. Journal of Non-Crystalline Solids, 2006, 352, 92-97.	1.5	9
119	A simple drain current model for Schottky-barrier carbon nanotube field effect transistors. Nanotechnology, 2007, 18, 419001.	1.3	9
120	Analysis of the breakdown spots spatial distribution in large area MOS structures. , 2010, , .		9
121	Nonhomogeneous spatial distribution of filamentary leakage current paths in circular area Pt/HfO2/Pt capacitors. Journal of Vacuum Science and Technology B:Nanotechnology and Microelectronics, 2013, 31, 01A107.	0.6	9
122	Modeling of the multilevel conduction characteristics and fatigue profile of Ag/La1/3Ca2/3MnO3/Pt structures using a compact memristive approach. Journal of Applied Physics, 2017, 121, .	1.1	9
123	SPICE modeling of cycle-to-cycle variability in RRAM devices. Solid-State Electronics, 2021, 185, 108040.	0.8	9
124	Lexicographic choice functions. International Journal of Approximate Reasoning, 2018, 92, 97-119.	1.9	9
125	An effective-field approach for the Fowler–Nordheim tunneling current through a metal–oxide–semiconductor charged barrier. Journal of Applied Physics, 1997, 82, 1262-1265.	1.1	8
126	Mesoscopic approach to progressive breakdown in ultrathin SiO2 layers. Applied Physics Letters, 2007, 91	1.5	8

#	Article	IF	CITATIONS
127	Electrical characterization of the soft breakdown failure mode in MgO layers. Applied Physics Letters, 2009, 95, 012901.	1.5	8
128	Degradation dynamics and breakdown of MgO gate oxides. Microelectronic Engineering, 2009, 86, 1715-1717.	1.1	8
129	Analysis of the breakdown spot spatial distribution in Pt/HfO2/Pt capacitors using nearest neighbor statistics. Journal of Applied Physics, 2013, 114, 154112.	1.1	8
130	Experimental Observation and Mitigation of Dielectric Screening in Hexagonal Boron Nitride Based Resistive Switching Devices. Crystal Research and Technology, 2018, 53, 1800006.	0.6	8
131	Conduction properties of breakdown paths in ultrathin gate oxides. Microelectronics Reliability, 2000, 40, 687-690.	0.9	7
132	Analytic model for the post-breakdown conductance of sub-5-nm SiO/sub 2/ gate oxides. IEEE Electron Device Letters, 2005, 26, 673-675.	2.2	7
133	Multiple Diode-Like Conduction in Resistive Switching SiO <italic>_x</italic> -Based MIM Devices. IEEE Nanotechnology Magazine, 2015, 14, 15-17.	1.1	7
134	Identification of the generation/rupture mechanism of filamentary conductive paths in ReRAM devices using oxide failure analysis. Microelectronics Reliability, 2017, 76-77, 178-183.	0.9	7
135	Exploratory study and application of the angular wavelet analysis for assessing the spatial distribution of breakdown spots in Pt/HfO2/Pt structures. Journal of Applied Physics, 2017, 122, 215304.	1.1	7
136	Simulation of Cycle-to-Cycle Instabilities in SiOx- Based ReRAM Devices Using a Self-Correlated Process with Long-Term Variation. IEEE Electron Device Letters, 2018, , 1-1.	2.2	7
137	Breakdown and anti-breakdown events in high-field stressed ultrathin gate oxides. Solid-State Electronics, 2001, 45, 1327-1332.	0.8	6
138	A drain current model for Schottky-barrier CNT-FETs. Journal of Computational Electronics, 2007, 5, 361-364.	1.3	6
139	Soft breakdown in MgO dielectric layers. , 2009, , .		6
140	Porosity enhancement by the utilization of screening patterns in electro-perforated paper webs. Journal of Electrostatics, 2010, 68, 196-199.	1.0	6
141	Modeling of the switching I-V characteristics in ultrathin (5 nm) atomic layer deposited HfO2 films using the logistic hysteron. Journal of Vacuum Science and Technology B:Nanotechnology and Microelectronics, 2015, 33, 01A102.	0.6	6
142	A thorough investigation of the progressive reset dynamics in HfO2-based resistive switching structures. Applied Physics Letters, 2015, 107, 113507.	1.5	6
143	Equivalent circuit model for the electron transport in 2D resistive switching material systems. , 2017, , \cdot		6
144	SPICE simulation of memristive circuits based on memdiodes with sigmoidal threshold functions. International Journal of Circuit Theory and Applications, 2018, 46, 39-49.	1.3	6

#	Article	IF	CITATIONS
145	Device variability tolerance of a RRAM-based self-organizing neuromorphic system. , 2018, , .		6
146	SPICE model for the current-voltage characteristic of resistive switching devices including the snapback effect. Microelectronic Engineering, 2019, 215, 110998.	1.1	6
147	Modeling of the temperature effects in filamentary-type resistive switching memories using quantum point-contact theory. Journal Physics D: Applied Physics, 2020, 53, 295106.	1.3	6
148	Application of the Clustering Model to Time-Correlated Oxide Breakdown Events in Multilevel Antifuse Memory Cells. IEEE Electron Device Letters, 2020, 41, 1770-1773.	2.2	6
149	Soft breakdown in irradiated high-Î $^{ m p}$ nanolaminates. Microelectronic Engineering, 2011, 88, 1425-1427.	1.1	5
150	Stress Conditions to Study the Reliability Characteristics of High-k Nanolaminates. ECS Transactions, 2012, 49, 161-168.	0.3	5
151	Compact analytical models for the SET and RESET switching statistics of RRAM inspired in the cell-based percolation model of gate dielectric breakdown. , 2013, , .		5
152	Failure Analysis of MIM and MIS Structures Using Point-to-Event Distance and Angular Probability Distributions. IEEE Transactions on Device and Materials Reliability, 2014, 14, 1080-1090.	1.5	5
153	Assessing the spatial correlation and conduction state of breakdown spot patterns in Pt/HfO2/Pt structures using transient infrared thermography. Journal of Applied Physics, 2014, 115, 174502.	1.1	5
154	SPICE Simulation of RRAM-Based Cross-Point Arrays Using the Dynamic Memdiode Model. Frontiers in Physics, 2021, 9, .	1.0	5
155	Two-step stress methodology for monitoring the gate oxide degradation in MOS devices. Solid-State Electronics, 2001, 45, 1317-1325.	0.8	4
156	BREAKDOWN MODES AND BREAKDOWN STATISTICS OF ULTRATHIN SiO ₂ GATE OXIDES. Selected Topics in Electornics and Systems, 2002, , 173-232.	0.2	4
157	Stochastic modeling of progressive breakdown in ultrathin SiO2 films. Applied Physics Letters, 2003, 83, 5014-5016.	1.5	4
158	Single-equation model for low and high voltage soft breakdown conduction. Microelectronics Reliability, 2004, 44, 163-166.	0.9	4
159	Electron transport through electrically induced nanoconstrictions in HfSiON gate stacks. Applied Physics Letters, 2008, 92, 253505.	1.5	4
160	Modeling of the Tunneling Current in MOS Devices After Proton Irradiation Using a Nonlinear Series Resistance Correction. IEEE Transactions on Nuclear Science, 2011, 58, 770-775.	1.2	4
161	From dielectric failure to memory function: Learning from oxide breakdown for improved understanding of resistive switching memories. , 2011, , .		4
162	Mesoscopic nature of the electron transport in electroformed metal-insulator-metal switches. Journal of Vacuum Science and Technology B:Nanotechnology and Microelectronics, 2011, 29, 01AD05.	0.6	4

#	Article	IF	CITATIONS
163	On the properties of conducting filament in ReRAM. , 2014, , .		4
164	Model for the Current–Voltage Characteristic of Resistive Switches Based on Recursive Hysteretic Operators. IEEE Electron Device Letters, 2015, 36, 944-946.	2.2	4
165	Resistive Switching: Coexistence of Grainâ€Boundariesâ€Assisted Bipolar and Threshold Resistive Switching in Multilayer Hexagonal Boron Nitride (Adv. Funct. Mater. 10/2017). Advanced Functional Materials, 2017, 27, .	7.8	4
166	Spatial analysis of failure sites in large area MIM capacitors using wavelets. Microelectronic Engineering, 2017, 178, 10-16.	1.1	4
167	SPICE simulation of 1T1R structures based on a logistic hysteresis operator. , 2017, , .		4
168	A new method for estimating the conductive filament temperature in OxRAM devices based on escape rate theory. Microelectronics Reliability, 2018, 88-90, 142-146.	0.9	4
169	Assessing the Correlation Between Location and Size of Catastrophic Breakdown Events in High-K MIM Capacitors. IEEE Transactions on Device and Materials Reliability, 2019, 19, 452-460.	1.5	4
170	Temperature Dependence of the Hard Breakdown Current of MOS Capacitors. , 2002, , .		3
171	Consistent model for the voltage and temperature dependence of the soft breakdown conduction mechanism in ultrathin gate oxides. Microelectronic Engineering, 2004, 72, 136-139.	1.1	3
172	Extraction of parameters and simulation of the hard breakdown I-V characteristics in ultrathin gate oxides. , 0, , .		3
173	Effects of the Semiconductor Substrate Material on the Post-breakdown Current of MgO Dielectric Layers. ECS Transactions, 2009, 25, 79-86.	0.3	3
174	Progressive breakdown dynamics and entropy production in ultrathin SiO2 gate oxides. Applied Physics Letters, 2011, 98, .	1.5	3
175	From post-breakdown conduction to resistive switching effect in thin dielectric films. , 2012, , .		3
176	Direct observation of the generation of breakdown spots in MIM structures under constant voltage stress. Microelectronics Reliability, 2013, 53, 1257-1260.	0.9	3
177	Analysis and Simulation of the Postbreakdown \$I-V\$ Characteristics of n-MOS Transistors in the Linear Response Regime. IEEE Electron Device Letters, 2013, 34, 798-800.	2.2	3
178	Breakdown time statistics of successive failure events in constant voltage-stressed Al2O3/HfO2 nanolaminates. Microelectronic Engineering, 2015, 147, 85-88.	1.1	3
179	Threading dislocations in III-V semiconductors: Analysis of electrical conduction. , 2015, , .		3
180	Electrical characterization of multiple leakage current paths in HfO2/Al2O3-based nanolaminates. Microelectronics Reliability, 2015, 55, 1442-1445.	0.9	3

#	Article	IF	CITATIONS
181	Characterization of the Failure Site Distribution in MIM Devices Using Zoomed Wavelet Analysis. Journal of Electronic Materials, 2018, 47, 5033-5038.	1.0	3
182	On the Application of a Diffusive Memristor Compact Model to Neuromorphic Circuits. Materials, 2019, 12, 2260.	1.3	3
183	Detection of inhibitory effects in the generation of breakdown spots in HfO2-based MIM devices. Microelectronic Engineering, 2019, 215, 111023.	1.1	3
184	Tunability Properties and Compact Modeling of HfOâ,,-Based Complementary Resistive Switches Using a Three-Terminal Subcircuit. IEEE Transactions on Electron Devices, 2021, , 1-8.	1.6	3
185	Assessment and Improvement of the Pattern Recognition Performance of Memdiode-Based Cross-Point Arrays with Randomly Distributed Stuck-at-Faults. Electronics (Switzerland), 2021, 10, 2427.	1.8	3
186	Analysis of the successive breakdown statistics of multilayer Al2O3/HfO2 gate stacks using the time-dependent clustering model. Microelectronics Reliability, 2020, 114, 113748.	0.9	3
187	Linear and non-linear conduction regimes in broken down gate oxides. Journal of Non-Crystalline Solids, 2001, 280, 132-137.	1.5	2
188	Experimental study and modeling of the temperature dependence of soft breakdown conduction in ultrathin gate oxides. , 0, , .		2
189	A new model for the breakdown dynamics of ultra-thin gate oxides based on the stochastic logistic differential equation. , 0, , .		2
190	Accurate assessment of the time-to-failure of hyper-thin gate oxides subjected to constant electrical stress using a logistic-type model. Microelectronic Engineering, 2005, 80, 166-169.	1.1	2
191	Simulation of the time-dependent breakdown characteristics of heavy-ion irradiated gate oxides using a mean-reverting Poisson-Gaussian process. IEEE Transactions on Nuclear Science, 2005, 52, 1462-1467.	1.2	2
192	Postbreakdown Current in MOS Structures: Extraction of Parameters Using the Integral Difference Function Method. IEEE Transactions on Device and Materials Reliability, 2006, 6, 190-196.	1.5	2
193	The Role of Power Dissipation on the Progressive Breakdown Dynamics of Ultra-Thin Gate Oxides. , 2007, , .		2
194	Analysis and modeling of the gate leakage current in advanced nMOSFET devices with severe gate-to-drain dielectric breakdown. Microelectronics Reliability, 2012, 52, 1909-1912.	0.9	2
195	Impact of the forming and cycling processes on the electrical and physical degradation characteristics of HfO2-based resistive switching devices. Thin Solid Films, 2020, 706, 138027.	0.8	2
196	A simple, robust, and accurate compact model for a wide variety of complementary resistive switching devices. Solid-State Electronics, 2021, 185, 108083.	0.8	2
197	Logistic model for leakage current in electrical stressed ultra-thin gate oxides. Electronics Letters, 2003, 39, 749.	0.5	2
198	Tunnelling in Al-silicon oxynitride-Si structures. Thin Solid Films, 1993, 230, 133-137.	0.8	1

#	Article	IF	CITATIONS
199	Impact of MOS technological parameters on the detection and modeling of the soft breakdown conduction. , 0, , .		1
200	Logistic modeling of progressive breakdown in ultrathin gate oxides. , 0, , .		1
201	Effect of the series resistance on the fowler-nordheim tunneling characteristics of ultra-thin gate oxides. , 0, , .		1
202	Modeling the Post-Breakdown Current in MOS devices on p-silicon substrate. , 2006, , .		1
203	Equivalent Electrical Circuit Model for the Post-Breakdown Current in SiO2/TiO2 Gate Stacks. , 2007, ,		1
204	Analytic Model for the Post-Breakdown Current in HfO <inf>2</inf> /TaN/TiN Gate Stacks. , 2007, , .		1
205	Analysis of the post-breakdown current in HfO2/TaN/TiN gate stack MOSFETs for low applied biases. Microelectronic Engineering, 2007, 84, 1960-1963.	1.1	1
206	Progressive breakdown dynamics in HfSiON/SiON gate stacks. , 2008, , .		1
207	Post-breakdown conduction in metal gate/MgO/InP structures. , 2009, , .		1
208	Effect of the Electric Discharge Confinement on the Perforation Density of Porous Materials. , 2010, ,		1
209	Parasitic back-inferface conduction in planar and triple-gate SOI transistors. , 2010, , .		1
210	Analytical modelling of Multiple-gate MOSFETs. , 2011, , .		1
211	Power-law logistic model for the current-time characteristic of metal gate/high-K/III-V semiconductor capacitors. , 2011, , .		1
212	Analysis of electroperforated materials using the quadrat counts method. Journal of Physics: Conference Series, 2011, 301, 012049.	0.3	1
213	Model for the leakage current decay in high-field stressed Al/HfYOx/GaAs structures. Microelectronic Engineering, 2011, 88, 1295-1297.	1.1	1
214	Application of the quadrat counts method to the analysis of the spatial breakdown spots pattern in metal gate/MgO/InP structures. Microelectronic Engineering, 2011, 88, 448-451.	1.1	1
215	Modeling the breakdown statistics of Al <inf>2</inf> O <inf>3</inf> /HfO <inf>2</inf> nanolaminates grown by atomic-layer-deposition. , 2011, , .		1
216	Model and Fitting Results for the Filamentary Conduction in MIM Resistive Switching Devices. ECS Transactions, 2011, 39, 187-193.	0.3	1

#	Article	IF	CITATIONS
217	Influence of Electrode Materials on CeOx Based Resistive Switching. ECS Transactions, 2012, 44, 439-443.	0.3	1
218	Spatial statistics for micro/nanoelectronics and materials science. , 2012, , .		1
219	Study of the spatial distribution of breakdown spots in MOS devices in case of important edge effect anomalies. , 2012, , .		1
220	Degradation and breakdown characteristics of Al/HfYOx/GaAs capacitors. Thin Solid Films, 2012, 520, 2956-2959.	0.8	1
221	Experimental evidence for a quantum wire state in HfO <inf>2</inf> -based VCM-RRAM. , 2013, , .		1
222	Field-effect control of breakdown paths in HfO2 based MIM structures. Microelectronics Reliability, 2013, 53, 1346-1350.	0.9	1
223	Modeling of the output characteristics of advanced n-MOSFETs after a severe gate-to-channel dielectric breakdown. Microelectronic Engineering, 2013, 109, 322-325.	1.1	1
224	Effect of an ultrathin SiO2 interfacial layer on the hysteretic current–voltage characteristics of CeOx-based metal–insulator–metal structures. Thin Solid Films, 2013, 533, 38-42.	0.8	1
225	Failure analysis of MIM and MIS structures using spatial statistics. , 2013, , .		1
226	Equivalent circuit model for the switching conduction characteristics of TiO <inf>2</inf> -based MIM structures. , 2014, , .		1
227	Investigation of switching mechanism in forming-free multi-level resistive memories with atomic layer deposited HfTiO <inf>x</inf> nanolaminate. , 2014, , .		1
228	Modeling of the conduction characteristics of voltage-driven bipolar RRAMs including turning point effects. , 2015, , .		1
229	Conduction and stability of holmium titanium oxide thin films grown by atomic layer deposition. Thin Solid Films, 2015, 591, 55-59.	0.8	1
230	Function-fit model for the rate of conducting filament generation in constant voltage-stressed multilayer oxide stacks. Journal of Vacuum Science and Technology B:Nanotechnology and Microelectronics, 2017, 35, 01A108.	0.6	1
231	Simple method for monitoring the switching activity in memristive cross-point arrays with line resistance effects. Microelectronics Reliability, 2019, 100-101, 113327.	0.9	1
232	An improved analytical model for the statistics of SET emergence point in HfO2 memristive device. AIP Advances, 2019, 9, 025118.	0.6	1
233	Natural Extension of Choice Functions. Communications in Computer and Information Science, 2018, , 201-213.	0.4	1
234	Compact Modeling and SPICE Simulation of GCMO-Based Resistive Switching Devices. IEEE Nanotechnology Magazine, 2022, 21, 285-288.	1.1	1

#	Article	IF	CITATIONS
235	Generation of electronic states at the silicon oxynitride-silicon interface in MOS structures. Journal of Physics Condensed Matter, 1993, 5, A319-A320.	0.7	0
236	Evaluation of the Degradation Dynamics of Thin Silicon Dioxide Films Using Model-Independent Procedures. Materials Research Society Symposia Proceedings, 1999, 592, 7.	0.1	0
237	A function-fit model for the hard breakdown l–V characteristics of ultra-thin oxides in MOS structures. Microelectronics Reliability, 2005, 45, 175-178.	0.9	0
238	A function-fit model for the hard breakdown l–V characteristics of ultra-thin oxides in MOS structures. Microelectronics Reliability, 2005, 45, 175-178.	0.9	0
239	Modeling of the Leakage Current in Ultrathin La2O3 Films Using a Generalized Power Law Equation. , 2006, , .		0
240	Post-breakdown conduction in ultra-thin HfO2 films in MOS transistors. Electronics Letters, 2007, 43, 1050.	0.5	0
241	Postbreakdown Conduction in Ultrathin \$hbox{La}_{2} hbox{O}_{3}\$ Gate Dielectrics. IEEE Transactions on Device and Materials Reliability, 2007, 7, 333-339.	1.5	0
242	Compact modeling of the non-linear post-breakdown current in thin gate oxides using the generalized diode equation. Microelectronics Reliability, 2008, 48, 1604-1607.	0.9	0
243	Compatibility of Co-Tunneling and Power-Law Models of Soft Breakdown Current in MOS Structures. , 2008, , .		0
244	Analysis and simulation of the post-breakdown leakage current in electrically stressed TiO2/SiO2 gate stacks. Thin Solid Films, 2009, 517, 1710-1714.	0.8	0
245	Exploratory analysis of the breakdown spots spatial distribution in metal gate/high-K/III–V stacks using functional summary statistics. Microelectronics Reliability, 2010, 50, 1294-1297.	0.9	0
246	Simulation of the Breakdown Spots Spatial Distribution in High-K Dielectrics and Model Validation Using the Spatstat Package for R Language. ECS Transactions, 2010, 33, 557-562.	0.3	0
247	Effects of High-Energy Ion Irradiation on the Conduction Characteristics of HfO2-based MOSFET Devices. ECS Transactions, 2010, 31, 327-332.	0.3	0
248	Simple model for the switching I-V characteristic in electroformed MIM structures. , 2010, , .		0
249	Toy model for the progressive breakdown dynamics of ultrathin gate dielectrics. , 2011, , .		0
250	A simple analytical and explicit compact model for the drain current of UTB SOI MOSFETs. , 2011, , .		0
251	Effect of the Electric Discharge Confinement on the Perforation Density of Porous Materials. IEEE Transactions on Industry Applications, 2011, 47, 2367-2373.	3.3	Ο
252	Method for improving the electrostatics perforation pattern using power controlled discharges. Journal of Physics: Conference Series, 2011, 301, 012016.	0.3	0

#	Article	IF	CITATIONS
253	Industrial electrostatics perforation improvement by power controlled discharges. , 2011, , .		0
254	Electrical evidence of atomic-size effects in the conduction filament of RRAM. , 2012, , .		0
255	Electron transport in CeO <inf>x</inf> -based resistive switching devices. , 2012, , .		Ο
256	Detection and characterization of the spatial inhibition potential in electroperforated sheet materials. Journal of Electrostatics, 2012, 70, 264-268.	1.0	0
257	Modeling of the post-breakdown I <inf>C</inf> -V <inf>C</inf> -V <inf>D</inf> characteristics of La <inf>2</inf> O <inf>3</inf> -based MOS transistors. , 2013, , .		Ο
258	Exploring the field-effect control of breakdown paths in lateral W/HfO <inf>2</inf> /W structures. , 2013, , .		0
259	Single-parameter model for the post-breakdown conduction characteristics of HoTiOx-based MIM capacitors. Microelectronics Reliability, 2014, 54, 1707-1711.	0.9	Ο
260	Modeling of the major and minor I-V loops in La0.3Ca _{0.7} MnO ₃ films using asymmetric logistic hysterons. , 2015, , .		0
261	Modeling of the I-V and I-t characteristics of multiferroic BiFeO <inf>3</inf> layers. , 2015, , .		0
262	The statistics of set time of oxide-based resistive switching memory. , 2016, , .		0
263	Electrical Properties and Nanoresistive Switching of Ni-HfO2-Si Capacitors. ECS Transactions, 2016, 72, 335-342.	0.3	0
264	Fabrication, characterization and modeling of TiN/Ti/HfO2/W memristors: programming based on an external capacitor discharge. , 2021, , .		0
265	Volume Resistive Switching in Metallic Perovskite Oxides Driven by the Metal-Insulator Transition. Kluwer International Series in Electronic Materials: Science and Technology, 2022, , 289-310.	0.3	0
266	Application of artificial neural networks to the identification of weak electrical regions in large area MIM structures. Microelectronics Reliability, 2021, , 114312.	0.9	0
267	Approximations of Coherent Lower Probabilities by 2-monotone Capacities. Communications in Computer and Information Science, 2018, , 214-225.	0.4	0
268	Failure Analysis of Large Area Pt/HfO2/Pt Capacitors Using Multilayer Perceptrons. , 2021, , .		0
269	SPICE Model for Complementary Resistive Switching Devices Based on Anti-Serially Connected Quasi-Static Memdiodes. Solid-State Electronics, 2022, , 108312.	0.8	0
270	Ternary Neural Networks Based on on/off Memristors: Set-Up and Training. Electronics (Switzerland), 2022, 11, 1526.	1.8	0

#	Article	IF	CITATIONS
271	Study of TiN/Ti/HfO2/W resistive switching devices: characterization and modeling of the set and reset transitions using an external capacitor discharge. Solid-State Electronics, 2022, , 108385.	0.8	0